ANTIOXIDANTS & REDOX SIGNALING
Volume 23, Number 12, 2015
DOI: 10.1089/ars.2014.6235

ORIGINAL RESEARCH COMMUNICATION

Converting a Sulfenic Acid Reductase into a Disulfide Bond Isomerase

Claire Chatelle,[1,*] Stéphanie Kraemer,[1,2,*] Guoping Ren,[1] Hannah Chmura,[1] Nils Marechal,[1] Dana Boyd,[3] Caroline Roggemans,[1,4] Na Ke,[1] Paul Riggs,[1] James Bardwell,[5] and Mehmet Berkmen[1]

Abstract

Aims: Posttranslational formation of disulfide bonds is essential for the folding of many secreted proteins. Formation of disulfide bonds in a protein with more than two cysteines is inherently fraught with error and can result in incorrect disulfide bond pairing and, consequently, misfolded protein. Protein disulfide bond isomerases, such as DsbC of *Escherichia coli*, can recognize mis-oxidized proteins and shuffle the disulfide bonds of the substrate protein into their native folded state. ***Results:*** We have developed a simple blue/white screen that can detect disulfide bond isomerization *in vivo*, using a mutant alkaline phosphatase (PhoA*) in *E. coli*. We utilized this screen to isolate mutants of the sulfenic acid reductase (DsbG) that allowed this protein to act as a disulfide bond isomerase. Characterization of the isolated mutants *in vivo* and *in vitro* allowed us to identify key amino acid residues responsible for oxidoreductase properties of thioredoxin-like proteins such as DsbC or DsbG. ***Innovation and Conclusions:*** Using these key residues, we also identified and characterized interesting environmental homologs of DsbG with novel properties, thus demonstrating the capacity of this screen to discover and elucidate mechanistic details of *in vivo* disulfide bond isomerization. *Antioxid. Redox Signal.* 23, 945–957.

Introduction

CORRECT DISULFIDE BOND FORMATION is essential for the folding and stability of numerous secreted proteins (2). As a result, cells have evolved dedicated enzymatic systems that catalyze their formation and isomerization (8). Most of these systems have thioredoxin-related thiodisulfide oxidoreductases (4). These proteins have various activities; thioredoxin serves mainly to reduce disulfides, DsbA to oxidize cysteines to disulfides, DsbC to isomerize disulfides, and DsbG to reduce sulfenic acid cysteine derivatives (6). Significant progress has been made in understanding the sequence and structural features that determine if a thioredoxin-related protein serves to oxidize, reduce, or isomerize disulfide residues (18), but little is known what distinguishes disulfide isomerases from proteins that are capable of sulfenic acid reduction.

DsbC, a homodimeric protein, has been shown *in vivo* and *in vitro* (45) to be an effective disulfide bond isomerase, both in the periplasmic (21) and cytoplasmic (20, 22) compartments. DsbG is a periplasmic oxidoreductase that shares 27% amino acid identity to DsbC. DsbG can function as a disulfide isomerase, although it is considerably weaker than DsbC both *in vivo* in facilitating the folding of urokinase (2) and *in vitro* in catalyzing the isomerization of scrambled hirudin (12, 14). In 2009, Depuydt *et al.* found that DsbG is a thiol protectant *in vivo*, reducing single cysteines from overoxidation (6). Recent studies have revealed that DsbC has a thiol protectant activity very similar to DsbG, but with a different substrate specificity (5).

[1]Protein Expression and Modification, New England Biolabs, Ipswich, Massachusetts.
[2]Actelion, Allschwil, Switzerland.
[3]Department of Microbiology and Immunobiology, Harvard Medical School, Boston, Massachusetts.
[4]Novartis, Basel, Switzerland.
[5]Howard Hughes Medical Institute Molecular, Cellular and Developmental Biology, University of Michigan, Ann Arbor, Michigan.
*These authors contributed equally to this work.

Innovation

Using these key residues, we also identified and characterized interesting environmental homologs of DsbG with novel properties, thus demonstrating the capacity of this screen to discover and elucidate mechanistic details of *in vivo* disulfide bond isomerization.

DsbC and DsbG exhibit similar activities under some conditions and different activities under others, depending on the substrate protein used in the study. For example, similar to DsbC, DsbG also has *in vitro* chaperone activity (36) and can assist in the folding of proteins *in vivo* when overexpressed (2, 49). Despite these similarities, these proteins have different capacities to protect cells against copper toxicity. Copper is a nonspecific thiol oxidant that catalyzes the formation of nonspecific non-native disulfide bonds in cells (30) resulting in cellular toxicity. The disulfide bond reductase/isomerase pathway is required to repair the oxidative damage caused by copper, presumably through reducing and removing non-native disulfide bonds and/or rearranging non-native disulfide bonds (13). Unlike DsbC, DsbG cannot protect cells against copper cytotoxicity. Previously, the copper-sensitive phenotype of *dsbC* null mutants was used to select mutations in the sulfenic acid reductase DsbG that conferred copper resistance (13). Numerous other structural differences exist, comparing DsbC and DsbG, and it is very difficult to determine just by inspection which of these multiple differences between the two proteins are responsible for the differences in activity.

In this study, we demonstrate the use of a simple blue/white screen capable of directly detecting disulfide bond isomerization *in vivo*. Unlike the previous screen based on isolating mutants of DsbG that alleviated a general copper-induced oxidative stress, in this article we present a new screen based on the folding of a mutant PhoA. Using this screen, we identify key residues that enhance the isomerase activity of DsbG in the cell, deepening our *in vivo* understanding of how disulfide bond isomerization enzymatic activity is determined.

Results

Detection of in vivo *periplasmic disulfide bond isomerase activity, using mutant PhoA**

We decided it would be useful to probe the *in vivo* mechanism of disulfide bond isomerization using a misoxidized protein, a mutant of periplasmic alkaline phosphatase. This mutant, PhoA*, lacks the first cysteine normally present in PhoA (C168S) and also contains an aberrant cysteine (S410C). Unlike for wild-type (wt) PhoA, correct disulfide bond formation in PhoA* requires linking cysteines that are nonconsecutive in sequence. PhoA* is initially misoxidized by the oxidase DsbA, which preferentially links consecutive cysteines. Its activity and folded state thus require the corrective action of the disulfide isomerase DsbC for proper folding (40). DsbG cannot catalyze the correct folding of PhoA*. This allows us to screen a plasmid library of DsbG* mutants for those that have gained the ability to fold PhoA* (39–41) (Fig. 1).

To confirm the dependence of PhoA* on DsbC for its activity, we cloned the gene encoding for *phoA** or wt *phoA* into the expression vector pBAD33. To avoid interference from chromosomally encoded alkaline phosphatase, all the strains used for the screen are *phoA* minus. We expressed the two proteins in strains lacking both the reductive pathway (*dsbC/dsbD*) and the oxidative pathway (*dsbA/dsbB*), in a single and pairwise manner, and measured the alkaline phosphatase activity from cell lysates by measuring hydrolysis of 4-nitrophenyl phosphate (pNPP) at 410 nm. As expected, wt PhoA was active when expressed in cells lacking the reductive/isomerase pathway (*dsbC* and/or *dsbD*) (Supplementary Fig. S1A; Supplementary Data are available online at www.liebertpub.com/ars). We also confirmed that PhoA* is ~5-fold less active than wt PhoA and is inactive when expressed in cells lacking the reductive/isomerase pathways (Supplementary Fig. S1B). Interestingly, wt PhoA is significantly more active in the Δ*dsbD* strain background, most likely due to increased levels of oxidized DsbC enhancing the capacity of the cells to correctly oxidize PhoA. Both PhoA constructs are inactive when expressed in cells lacking the oxidative pathway (*dsbA* and/or *dsbB*).

The dependence of PhoA* on the *dsbC/dsbD* pathway indicated that the homolog of DsbC and DsbG is not sufficient to allow for the isomerization of disulfide bonds in PhoA*. DsbG is normally expressed at a level only 20% of that of DsbC (51, 52). To test whether overexpressed DsbG can assist in the folding of PhoA*, we cloned *dsbG* into a multicopy expression vector, pMER79 (38). The native signal sequence of *dsbG* on this plasmid was replaced with that of the signal recognition particle (SRP)-dependent signal sequence of *torT* (34) along with a 3′ flag tag sequence. By replacing the sec-dependent signal peptide of DsbG with that of an SRP-dependent signal peptide of DsbA, we hoped to circumvent mutations that may alter the secretion of DsbG*.

To monitor the folding and expression of PhoA* in the presence of overexpressed DsbC or DsbG, we transformed cells lacking *dsbC* and harboring pBAD33-phoA* with the following: (i) an empty expression control vector, (ii) the vector expressing *dsbC*, or (iii) the vector expressing *dsbG*-flag. We grew the three strains on minimal agar plates that contain 5-bromo-4-chloro-3-indolyl phosphate (XP), which is an artificial substrate of PhoA. Strains that can hydrolyze XP form blue colonies, whereas strains that cannot, form opaque ecru colonies. Extensive optimization of each media component and expression condition was required to achieve the ideal time to detect the difference between blue and ecru colonies (Supplementary Fig. S2).

We found that cells expressing DsbC formed blue colonies, indicating that the PhoA* was functional. In contrast, cells expressing DsbG-flag or the empty vector formed opaque ecru colonies, indicating that DsbG-Flag cannot functionally substitute for DsbC to fold PhoA*, even when overexpressed from a multicopy plasmid.

Selection of mutant DsbG capable of folding PhoA**

The inability of DsbG to isomerize PhoA* allowed us to use this as a screen to identify DsbG variants (designated DsbG*) that can fold PhoA*. We transformed Δ*dsbC* Δ*phoA* cells expressing PhoA* (MB1045) with a plasmid library of *dsbG** mutants. We screened a total of 30,000 transformants on 3-(*N*-morpholino)propanesulfonic acid (MOPS)-XP plates after incubation for 2 days at 30°C. The phenotypes of

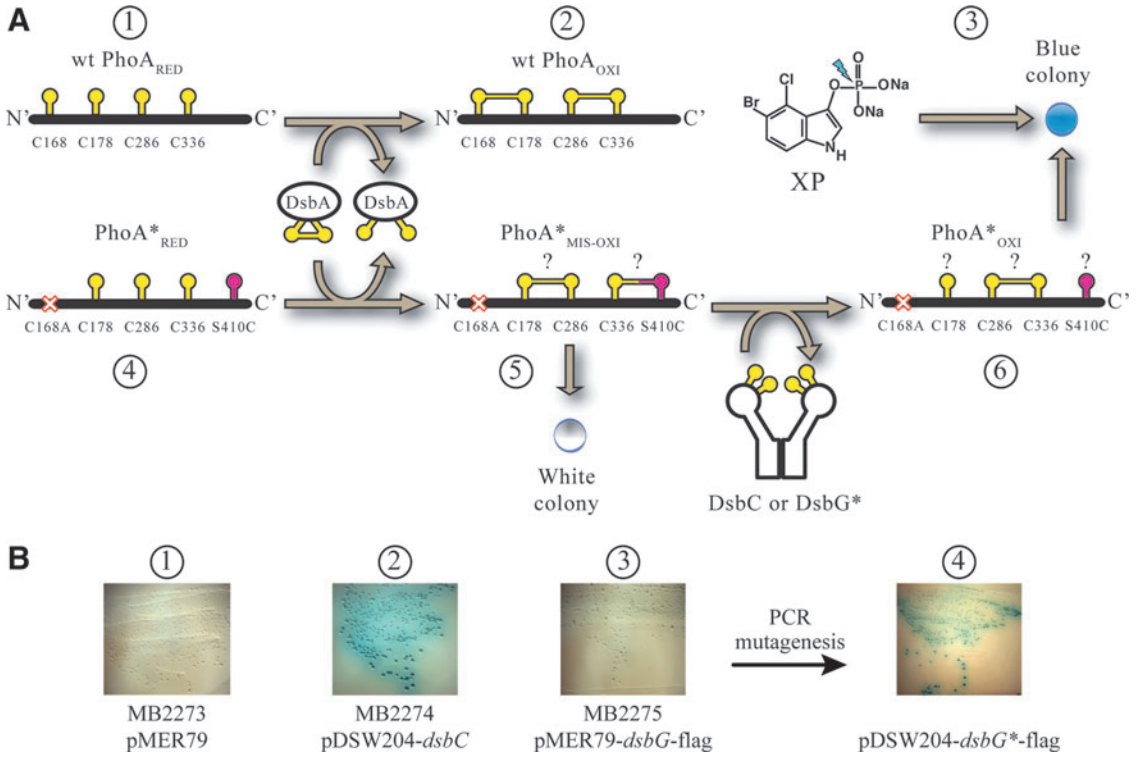

FIG. 1. Principle of *in vivo* disulfide bond isomerase screen using mutant PhoA*. (A) ① Reduced wt alkaline phosphatase (wt $PhoA_{RED}$) with four cysteines (*yellow balls* with *numbers* indicating cysteine residue) is correctly oxidized by DsbA to form two consecutive disulfide bonds. ② Active folded PhoA (wt $PhoA_{OXI}$) can hydrolyze XP, ③ resulting in *blue* colonies. ④ Reduced mutant alkaline phosphatase ($PhoA^*_{RED}$) lacking the first cysteine (C168A) and with an additional mutant cysteine (S410C in magenta) is mis-oxidized by DsbA ($PhoA^*_{MIS-OXI}$), resulting in unknown disulfide bond pattern. ⑤ Colonies expressing inactive misfolded PhoA*, which cannot hydrolyze XP, remain their natural *white* color. ⑥ Misfolded PhoA* is isomerized by DsbC or DsbG* mutants to an active form ($PhoA^*_{OXI}$) with an unknown disulfide bond pattern resulting in *blue* colonies. **(B)** Selection of DsbG* mutants on MOPS-XP plates. ① Cells lacking *dsbC*, *dsbG*, *phoA* and harboring an empty expression vector along with pBAD33-PhoA* are *opaque* and *ecru* when plated on the selective MOPS-XP media. ② Cells turn *blue* when expressing DsbC from the plasmid pDSW204. ③ Cells remain *ecru* when expressing DsbG from the plasmid pMER79. ④ PCR mutagenized library of pMER79-*dsbG**-flag, transformed into cells lacking *dsbC*, *dsbG*, *phoA*, and *blue* colonies, which have active folded PhoA*, was selected. MOPS, 3-(*N*-morpholino)propanesulfonic acid; PCR, polymerase chain reaction; wt, wild type; XP, 5-bromo-4-chloro-3-indolyl phosphate.

small faint-blue colonies were confirmed by restreaking on MOPS-XP plates. Plasmid DNA from the positive clones was transformed into a *dsbC*, *dsbG* null strain expressing *phoA** (MB2272) to confirm that the blue colony phenotype was linked to the plasmid and not the host strain. From the 48 *dsbG** candidates sequenced, we recloned 18 of them into the parental vector to avoid any plasmid backbone-linked phenotype and then resequenced them. The final 18 mutant *dsbG** candidates identified are listed in Supplementary Table S1.

The DsbG structure is composed of a thioredoxin-like domain connected to a dimerization domain through a 24 amino acid linker. We mapped the location of the mutations to each of these three domains of DsbG. We analyzed the change in charge, which occurred due to the mutation, to evaluate whether the mutations increased or decreased the charge in the cleft between the two monomers of DsbG (the cleft in DsbG is more charged compared with DsbC). Finally, we analyzed each mutation using the web-based ConSurf software, which measures the degree to which a residue is conserved among both DsbC and DsbG homologs as a way to first gauge how important that residue is to the structure and/or function of the combined DsbC/G isomerase family and then to separately gauge how conserved it was within the individual DsbC and DsbG families.

To confirm that the DsbG* mutants can fold PhoA*, we conducted alkaline phosphatase assays on cells expressing both PhoA* and the selected 18 DsbG* candidates (Supplementary Fig. S3). As expected, the strain expressing DsbC was able to correctly fold PhoA*, resulting in high alkaline phosphatase activity. Ten of the *dsbG** candidates carried single mutations and 8 carried two to six mutations, with an overall average of 2.2 amino acid substitutions per *dsbG** gene. For those that contained single substitutions, we can be reasonably certain that these mutations are sufficient to confirm the increased PhoA* activity. For those that contained multiple mutations, the individual mutations could all contribute in an additive manner or some of these mutations could be silent or partially deleterious. The three DsbG variant strains that expressed the highest level of PhoA* contained three to six mutations suggesting that in these cases more than one mutation may contribute to their strong phenotype. Interestingly, several of the residues mutated in our selection (K113N, N198I, and T211S) had been previously found using the copper selection (K113E/N, N198Y/I, and

T211R/M) (14) (see Introduction section). K113N, for instance, was present in the DsbG variant that conferred the second highest level of PhoA* activity and also had been isolated multiple times as copper-resistant mutations. However, the remainder of the DsbG* variants isolated with the PhoA* screen was different from those isolated through copper resistance, suggesting that the two procedures selected for at least slightly different activities. Expression of DsbG* variants resulted in PhoA* activity up to 70% of that found in strains wild type for DsbC, suggesting that we had obtained DsbG variants that could effectively replace DsbC (Supplementary Fig. S3A). Surprisingly, while the entire mutant DsbG*s selected and retransformed were confirmed to be bluer than wt DsbG, expression of five mutants resulted in PhoA* activities that were close to or below the levels observed with wt DsbG. Although these results suggest that the PhoA* selection scheme results in few false positives, the use of two different substrates, XP and pNPP, for the analysis of activity in solid *versus* liquid media may explain the differences in the PhoA* activity and/or folding.

To evaluate whether the 18 DsbG* mutants were specific to folding only PhoA* or if they were also capable of folding other proteins that required disulfide isomerization, we transformed Δ*dsbC* cells expressing phytase (*appA*) with each of the 18 *dsbG** plasmids. AppA is an *Escherichia coli* periplasmic enzyme containing three consecutive and one nonconsecutive disulfide bond. Folding of AppA is dependent on the disulfide bond isomerase activity of DsbC (1). However, the folding of AppA is not specific to DsbC, as AppA can fold efficiently (~90%) when wt DsbG is overexpressed. Expression of the 18 *dsbG** plasmids generally resulted in 60–90% AppA activity, indicating that nearly all of the DsbG* variants are still proficient in folding of AppA and have, therefore, not lost their isomerase/chaperone function (Supplementary Fig. S3B). The only apparent exception was DsbG*$_{63}$, which complemented the folding of AppA at levels only 40% that of DsbC (Supplementary Fig. S3B, lane 6).

A single-point mutation in DsbG is sufficient to gain the ability to facilitate the folding of PhoA**

The initial screen on MOPS-XP plates identified many DsbG* mutants capable of folding PhoA*. We selected three DsbG* mutants (DsbG*$_2$, DsbG*$_{50}$, and DsbG*$_{72}$) for further characterization, as their expression either resulted in the greatest improvements in the folding of PhoA* (85% DsbG*$_2$, 75% DsbG*$_{50}$ activity in relation to DsbC) (Fig. 2B) or was potent in the ability of DsbG to rescue from copper toxicity (DsbG*$_{72}$ protection against copper was equal to DsbC) (Fig. 2C). These mutants carried multiple amino acid substitutions (DsbG*$_2$: L43Q, K113N, Q214R; DsbG*$_{50}$: A5S, K8T, F21L, L169P, D193G, Q214R; and DsbG*$_{72}$: K19R, T44S, Y56F, V199A, T211S). To identify critical residues involved in disulfide bond isomerization, we engineered 13 DsbG* mutants, each having one of the mutations from the three selected mutants. We were particularly interested in two of these mutations: (i) Q214R because it was present both in DsbG*$_2$ and DsbG*$_{50}$ and (ii) K113N because it was present in DsbG*$_2$ and had previously been shown to be effective in allowing DsbG to confer protection against copper toxicity (14).

To evaluate the *in vivo* disulfide bond isomerase activity of the three selected mutants (DsbG*$_{50}$, DsbG*$_2$, and DsbG*$_{72}$) and the engineered 14 DsbG* mutants with single amino acid substitutions, the PhoA* activity was determined from crude lysates of Δ*dsbC* Δ*dsbG* cells expressing PhoA* and various DsbG* mutants (Fig. 2A). Strains expressing most of the mutant DsbG*s showed a PhoA* activity equal to or higher compared with a strain overexpressing wt DsbG. Strains expressing DsbG*$_{50}$ and DsbG*$_2$ displayed the highest PhoA* activity, while the strain expressing DsbG*$_{72}$, which confers a high level

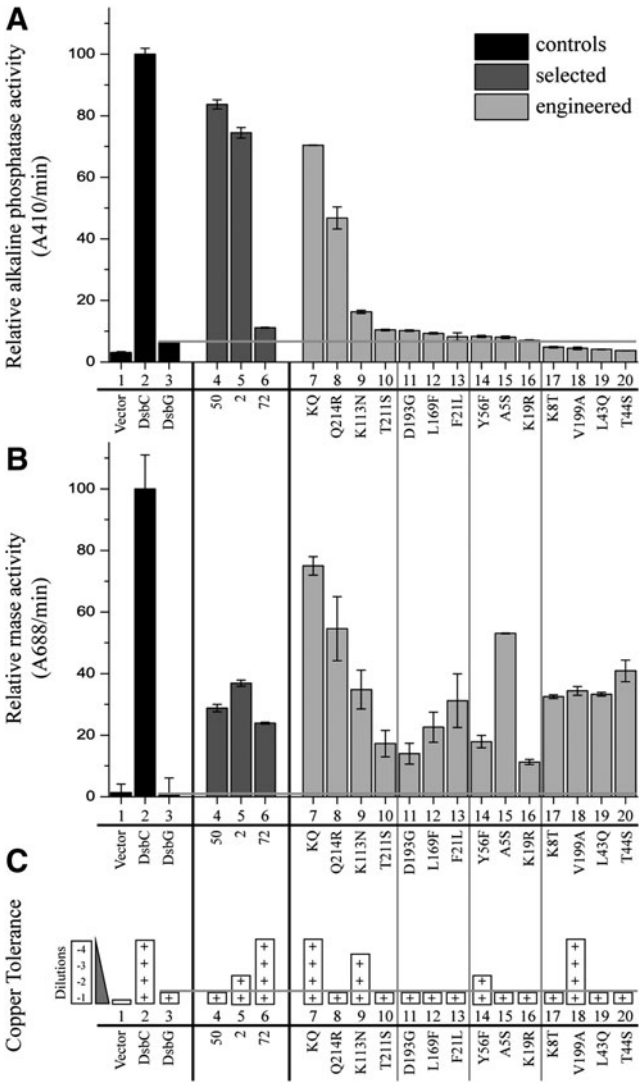

FIG. 2. *In vivo* activities of DsbG* mutants. Cells expressing PhoA* or RNase I from pBAD33 and DsbC/DsbG/DsbG* from pMER79 were grown in M63 minimal media until mid-log phase. All activities were normalized to cells expressing DsbC. Control constructs (*lanes 1–3*, *black bars*), selected DsbG* mutants (*lanes 4–6*, *dark gray bars*), and engineered DsbG* mutants (*lanes 7–20*, *light gray bars*) are indicated. **(A)** *In vivo* alkaline phosphatase activity. Phosphatase activities from whole cells were measured as an increase in the rate of absorbance at 410 nm, using pNPP. **(B)** *In vivo* RNase activity. RNase activities from soluble lysates were measured as a decrease in the rate of absorbance at 688 nm, in a methylene blue assay. **(C)** *In vivo* copper toxicity protection. Cells were serially diluted, spotted on BHI plates supplemented with 9 m*M* $CuSO_4$, and grown for 2 days at 30°C. BHI, brain heart infusion; pNPP, 4-nitrophenyl phosphate; RNase I, ribonuclease I.

of copper resistance, showed a PhoA* activity of only 11%. Of the engineered single mutants, expression of DsbG*$_{Q214R}$ resulted in an eightfold higher PhoA* activity compared to wt DsbG, while expression of DsbG*$_{K113N}$ resulted only in a twofold improvement. However, this mutant still remained lower than the original multimutant parental DsbG* (DsbG*$_{50}$ and DsbG*$_{2}$), suggesting multiple mutations are necessary to convert DsbG into an efficient disulfide bond isomerase that is capable of folding PhoA*. Nevertheless, a single-point mutation Q214R in DsbG is sufficient to make the enzyme partially able to fold PhoA* (Fig. 2A, lane 8) into its native active structure. This effect was further enhanced with the addition of the critical K113N mutation, resulting in a double mutant named DsbG*$_{KQ}$ (Fig. 2A, lane 7).

DsbG mutants can assist folding ribonuclease I, a native substrate of DsbC*

The DsbG* mutants were selected for their ability to fold the artificial DsbC substrate PhoA*. It is conceivable that mutations are specific to folding PhoA* and have not converted DsbG* to a general disulfide bond isomerase. To evaluate the substrate specificity of the selected DsbG*s, we performed a third *in vivo* disulfide bond isomerase activity assay using a natural substrate of DsbC, ribonuclease I (RNase I). *E. coli* periplasmic RNase I contains four disulfide bonds, including a nonconsecutive one, making its folding dependent on DsbC (12, 26). To evaluate the disulfide bond isomerase activity of DsbG* mutants, we used a methylene blue assay to measure RNase I activity from lysates made from Δ*dsbC* Δ*dsbG* cells overexpressing periplasmic RNase I as well as various DsbG* mutants (Fig. 2B).

The RNase I activity in cells overexpressing wt DsbG from a plasmid was 5%, barely above cells with an empty vector (3%), whereas overexpression of DsbC was sufficient to restore the RNase I activity (100%). Overexpression of all DsbG* mutants resulted in a significant increase in RNase I folding, although these activities, which ranged from 15% to 70%, did not reach the 100% level found in the strain overexpressing DsbC. These results indicate that the selected mutations in DsbG* obtained from the PhoA* screen confer a general disulfide bond isomerization activity; they are not specific for the ability to fold only the artificial DsbC substrate PhoA*, but can also assist in the folding of a natural substrate, RNase I.

DsbG mutants confer protection against copper cytotoxicity*

Previously, the copper-sensitive phenotype of *dsbC* null mutants was used to select mutations in DsbG that conferred copper resistance (13). A number of these copper-resistant DsbG mutants showed enhanced isomerase activity. Interestingly, several of the residues mutated in our selection (K113E/N, N198Y/I, and T211R/M) had been previously found in this copper resistance selection (K113N, N198I, and T211S) (14). K113N, for instance, was present in the DsbG variant that conferred the second highest level of PhoA* activity and also had been isolated multiple times as copper-resistant mutations. However, the remainder of the DsbG* variants isolated with the PhoA* screen was different from those isolated through copper resistance, suggesting that the two procedures were selected for at least slightly different activities. To further evaluate the *in vivo* disulfide bond reductase/isomerase activity of the DsbG* mutants isolated with the PhoA* screen, we plated out serial dilutions of Δ*dsbC* Δ*dsbG* cells harboring various DsbG mutants in minimal M63 media and plated them out in serial dilutions on brain heart infusion (BHI) agar plates supplemented with 9 m*M* copper. We compared the growth of strains harboring DsbG* mutants to strains with wt DsbG or DsbC (Fig. 2C). As expected, cells overexpressing DsbC grew in the presence of copper, whereas cells overexpressing wt DsbG or containing an empty vector did not. Two of our 18 DsbG*-selected mutants (DsbG*$_{2}$ and DsbG*$_{72}$) protected cells at significant levels from copper toxicity. Not surprisingly, these mutants contained residues that when mutated had previously been shown to cause copper resistance (Supplementary Fig. S4).

Among these two DsbG* mutants, only DsbG*$_{72}$ (Fig. 2C, lane 6) provided full protection against copper toxicity similar to DsbC. Partial protection was observed for DsbG*$_{2}$ and for the engineered DsbG*$_{K113N}$ and DsbG*$_{Y56F}$ (Fig. 2C, lane 5, 9, and 14). Both DsbG*$_{K113N}$ and DsbG*$_{2}$ contain mutations previously associated with copper resistance, but DsbG*$_{Y56F}$ does not. Interestingly, expression of the engineered double mutant DsbG*$_{KQ}$ further enhanced the copper protection capacity of DsbG*$_{K113N}$ and resulted in DsbC-like copper toxicity protection. Surprisingly, DsbG*$_{V199A}$ provided full protection against copper toxicity (Fig. 2C, lane 18) compared to partial protection by DsbG*$_{K113N}$, which had previously been selected specifically for copper toxicity protection (13). The copper-resistant mutants were selected to alleviate general overoxidation in the periplasm and not to fold and isomerize a specific protein.

In conclusion, our screen identified new DsbG mutations that confer general capacity to protect cells against copper-induced mis-oxidation and fold mis-oxidized proteins that are not specific to folding PhoA*. The additional mutations isolated in our screen indicate that the mutant landscape of DsbG was wider than previously appreciated.

Key residues identified in PhoA screen can help discover DsbG homologs with novel properties*

The PhoA* screen identified several residues important in modulating the redox activities of DsbG. Homologs having the same substitutions that could, in theory, exist in nature, and the amino acid substitutions identified in our screen could represent the functional and biological diversity of DsbC/G-like proteins. To test this hypothesis, we analyzed DsbC and DsbG homologs identified in sequenced bacterial genomes and asked whether any homolog contained any of the three key residues (N113, R214, and A199) identified in the PhoA* screen. We used a hidden Markov model to predict which of the ~390 homologs (Supplementary Table S2) were DsbC like or DsbG like and conducted further characterization on the topology, active site, and phylogeny of the homologs (Supplementary Fig. S5). Using this list, we searched for homologs of DsbG that naturally contained residues identified in our screen to be critical (Supplementary Table S3).

We found a homolog of DsbG in *Thiobacillus denitrificans* ATCC 25259 that contained the key residue N113, shown to confer protection against copper toxicity in DsbG*$_{K113N}$ (Supplementary Fig. S6A). *T. denitrificans* also has been previously identified to be resistant to copper and has been used in bioremediation for the removal of metals (42). We therefore postulated that unlike *E. coli* DsbG (DsbG$_{Ec}$), since

the *T. denitrificans* DsbG ($DsbG_{Td}$) has an N at the key 113th residue, its residue should confer copper resistance and be able to fold PhoA*. We performed alkaline phosphatase activity and copper protection assays with Δ*dsbC* Δ*dsbG* Δ*phoA E. coli* cells expressing PhoA* along with $DsbG_{Td}$, $DsbG_{Ec}$, $DsbG^*_{K113N}$, or $DsbG^*_{KQ}$. $DsbG_{Td}$ gave higher PhoA* activity compared to $DsbG^*_{K113N}$ and equal to $DsbG^*_{KQ}$ (Supplementary Fig. S6B). As predicted, $DsbG_{Td}$, $DsbG^*_{K113N}$, and $DsbG^*_{KQ}$ provided similar levels of protection against copper toxicity (Supplementary Fig. S6C). These results indicate that key residues identified in modulating DsbG activity can be used to discover oxidoreductases with novel properties. We postulate that the N113 mutation in $DsbG_{Td}$ could contribute, at least in part, to the ability of *T. denitrificans* to resist copper. Our identification of key residues that appear to modulate the DsbG activity may be useful in predicting the property of DsbG homologs.

In vitro *oxidoreductase properties of DsbG* mutants*

The DsbG* mutants isolated from the PhoA* screen have significant differences in their *in vivo* substrate specificity and in their capacity to protect cells from copper toxicity. To further our understanding on the effects of the mutations on DsbG's oxidoreductase properties, we compared the *in vitro* redox activities of purified DsbG* mutants to wt DsbG and DsbC. We focused our studies on the original screen mutants, $DsbG^*_2$, $DsbG^*_{50}$, and $DsbG^*_{72}$, and on the engineered mutants, $DsbG^*_{KQ}$, $DsbG^*_{Q214R}$, $DsbG^*_{K113N}$, and $DsbG^*_{V199A}$. We performed three different *in vitro* assays to biochemically characterize their capacities to (i) reduce disulfide bonds, (ii) oxidize cysteines, and (iii) isomerize incorrect disulfide bonds (Fig. 3).

In our first biochemical assay, we assayed the ability of DsbG* mutants to reduce disulfide bonds using an insulin reductase assay. We found that DsbG and its variants have negligible insulin reductase activity *in vitro*, ~1000-fold less than DsbC (Fig. 3A). We conclude that the DsbG* mutants like wt DsbG function very poorly as disulfide bond reductases *in vitro*.

In the second biochemical assay, we determined the ability of the mutants to oxidize cysteines by conducting hirudin oxidase assays. We monitored oxidation of fully reduced hirudin by DsbG and its variants *in vitro* by fluorescence excitation at 295 nm, which increases when oxidized DsbG

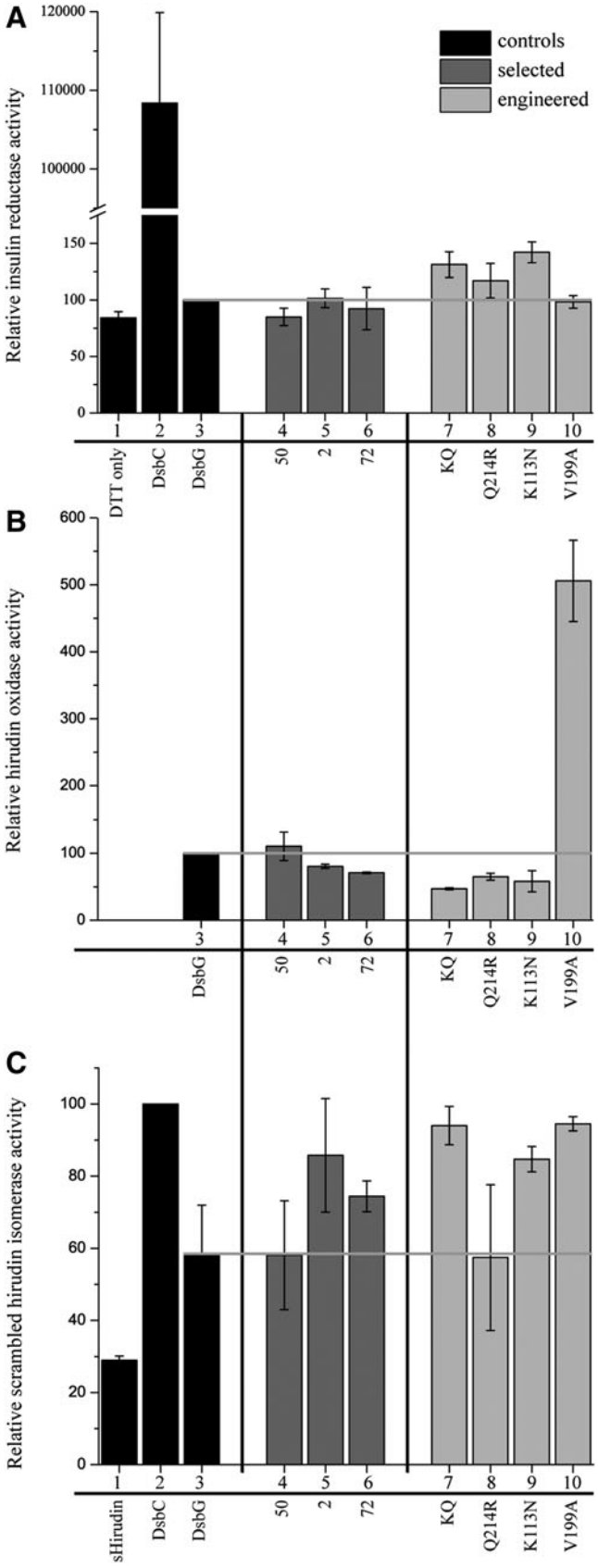

FIG. 3. *In vitro* activities of DsbG* mutants. Purified DsbC/DsbG/DsbG* samples were subjected to various *in vitro* assays. Negative control samples without protein, wt DsbC and wt DsbG control samples are shown as *black bars* (*lanes 1–3*). Selected DsbG* mutants (*lanes 4–6*, *dark gray bars*) and engineered DsbG* mutants (*lanes 7–10*, *light gray bars*) are indicated. **(A)** Disulfide bond reductase activity. Protein samples were incubated with disulfide-bonded insulin and the rate of its reduction was followed at 650 nm in the presence of DTT. **(B)** Disulfide bond oxidase activity. Protein samples were incubated with fully reduced hirudin and the increase in DsbG fluorescence excitation at 295 nm was monitored over time. **(C)** Disulfide bond isomerase activity. Protein samples were incubated with scrambled hirudin and the folding of correctly folded hirudin was measured by HPLC. *Horizontal gray bar* indicates level of activity observed for wt DsbG. DTT, dithiothreitol; HPLC, high-performance liquid chromatography.

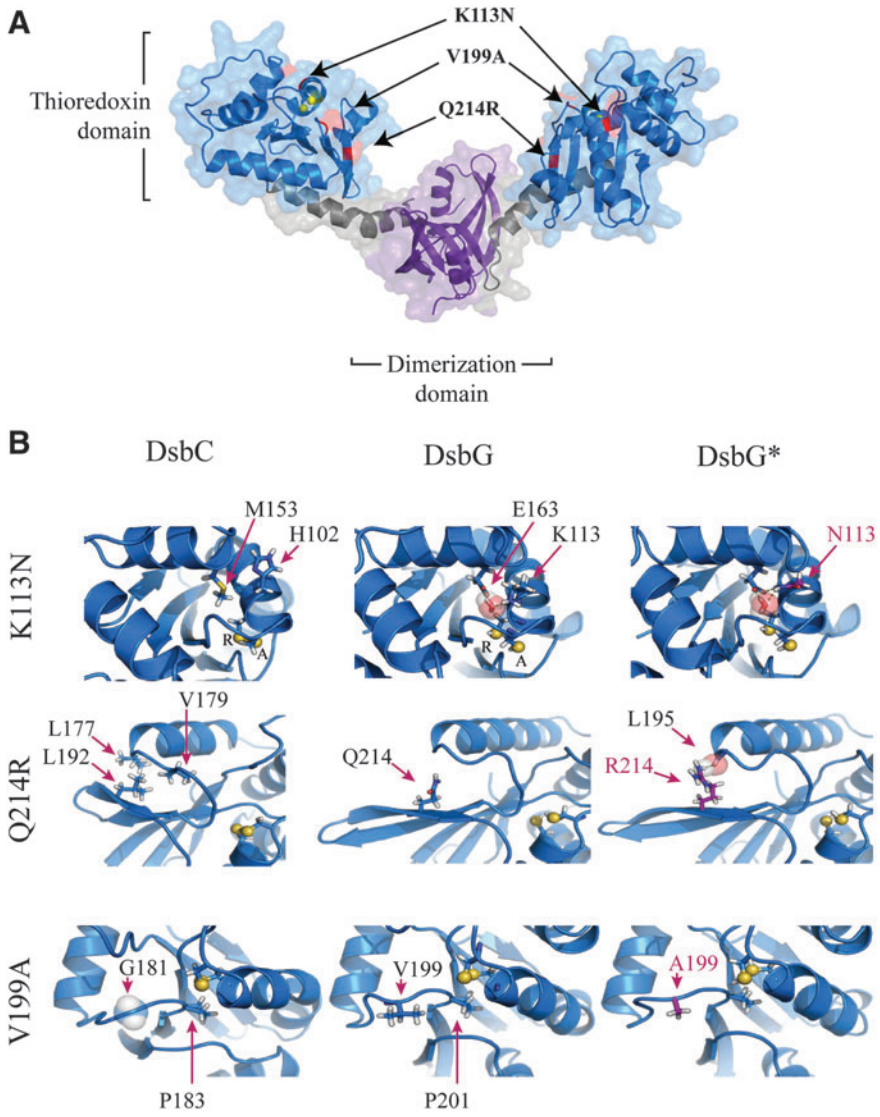

FIG. 4. Structural locations of mutations isolated in DsbG*. (A) DsbG homodimer is shown with the thioredoxin (*blue*) and dimerization (*purple*) domains highlighted. The alpha-helical linker is shown in *gray*. The locations of the three substitutions (*red*) are shown in each dimer with *arrows*. **(B)** Close-up structures of the wt DsbC and DsbG and the modeled DsbG* are shown. PyMOL predicted structures of mutant residues (*purple*), and wt residues (*black*) are shown. The active site cysteines are shown as *yellow balls* and the resolving (R) and attacking (A) cysteines are indicated.

donates its disulfide bond to hirudin. DsbC-catalyzed hirudin oxidation cannot be measured because the tryptophan fluorescence of DsbC does not correlate with its active-site disulfide bond redox status (47). Our results indicate that neither wt DsbG nor the vast majority of DsbG* variants can efficiently catalyze the oxidation of hirudin *in vitro* (Fig. 3B). The only exception was DsbG*$_{V199A}$, which displayed a significant (~5-fold) more rapid change in fluorescence compared to wt DsbG, when incubated with reduced hirudin (Fig. 3B, lane 10).

The *in vitro* oxidase activity of DsbG*$_{V199A}$ indicated that perhaps the *in vivo* folding of PhoA* is due to its correct oxidation by DsbG*$_{V199A}$, before its mis-oxidation by DsbA. To test the hypothesis that the DsbG* mutants could properly oxidize and fold PhoA* in the absence of both DsbA and DsbC, we grew Δ*dsbC* Δ*dsbA* cells expressing PhoA* along with the selected DsbG* variants in minimal media and assayed the phosphatase activity from whole cells (Supplementary Fig. S7). Expression of DsbG* mutants resulted in a significantly higher activity of PhoA* compared to the background oxidation of cells expressing wt DsbG from the same vector (Supplementary Fig. S7, lane 3). The only exception was DsbG*$_{72}$, which did not, however, it was not isolated for an ability to fold PhoA*, but rather for its ability to protect cells against copper-induced toxicity. Notably, none of the DsbG* mutants was as efficient as wt cells (*dsbA*$^+$ *dsbC*$^+$) in expressing PhoA* *in vivo* (Supplementary Fig. S7, lane 1). This indicates that DsbG* alone is insufficient for the correct folding of PhoA*.

In our third biochemical assay, we determined whether the purified DsbG* mutants could isomerize disulfide bonds *in vitro* by incubating equal molar quantities of scrambled hirudin and purified DsbG and variants. We quenched the reaction by acid and quantified the amount of correctly folded hirudin using high-performance liquid chromatography (HPLC) (Fig. 3C). In the absence of any added disulfide oxidoreductase, we found that ~30% of the hirudin had attained its correctly folded state (Fig. 3C, lane 1). Upon incubation with DsbC, we detected almost all of the scrambled hirudin in its correctly folded state, compared to only ~60% in its correctly folded state when incubated with wt DsbG (Fig. 3C, lane 2 and 3). The majority of the DsbG* mutants appeared to improve the folding of hirudin slightly, compared to wt DsbG (ranging from ~75% to ~95%). Only mutants

$DsbG^*_{50}$ and $DsbG^*_{Q214R}$ did not show any improvement in their capacity to isomerize scrambled hirudin.

Structural analysis of the DsbG mutants (K113N, V199A, Q214R)*

We mapped the three mutations Q214R, K113N, V199A that we identified as being critical for the modulation of DsbG isomerase activity on the crystal structure of DsbG (PDB# 1V58) (11) and conducted *in silico* modeling of the substitutions using PyMOL (35). Both V199 and K113 are in close proximity to the active site $C_{109}XXC_{112}$, while Q214 is facing the cleft formed between the two subunits of DsbG (Fig. 4A). The alignment between modeling output and crystal structures results in a RMSD of 0.62 Å with none of the substitutions significantly affecting the overall fold.

$DsbG_{K113N}$. Modeling of the K113N substitution predicted that the hydrogen bond network involving a water molecule stabilized by K113 and E163 in wild-type DsbG is retained in $DsbG_{K113N}$ (Fig. 4B). However, the shorter asparagine side chain creates a small cleft exposing the charge of the E163 carboxyl group. A short 0.1 ns dynamics simulation (data not shown) suggests that the solvent can enter this cavity and disturb the E163-H2O-N113 hydrogen bond network. These residues are located near the resolving active site C112 and could be involved in electron/proton transfers between the solvent and the buried C112 in the active site. It has been previously shown that the ionizable residues in a buried environment can impact cysteine pK_a values and, thus, affect cysteine reactivity (7). Replacing the ionizable K113 with a polar, uncharged asparagine residue could modify the physicochemical properties of the environment surrounding the CXXC active site. In DsbC, this environment is mainly composed of hydrophobic residues (the E163-H2O-K113 bridge position is occupied by MET153 εCH_3). Thus, we assume that K113N mutation in DsbG could modify the CXXC activity in a DsbC-like way. This could explain the enhancement in $DsbG_{K113N}$ *in vitro* reductase activity and its improved capacity to protect against copper-induced cytotoxicity.

$DsbG_{V199A}$. The V119A substitution occurs on the loop that contains the highly conserved cis-proline 201, known to play a critical role in the activity and substrate release kinetics of oxidoreductases (19, 29). The modeling result suggests that V199A substitution adopts the same orientation as in wt DsbG and is in the −2 position in relation to the cis-P201. The V199A substitution lowers steric contacts between the cis-proline loop and surrounding amino acids, enhancing the flexibility of this loop in a DsbC-like manner. This increased flexibility would change the P201 dynamics, in direct contact with the resolving cysteine in the CXXC active site. Similar observations have been made for mutations in the −1 position of the cis-proline, which modulate the oxidoreductase properties of thioredoxin (24, 29). In DsbC, DsbA, and TrxA, a glycine residue occupies the equivalent −2 position. Our observations are the first example of a mutation that modulates the activity of an oxidoreductase, in the −2 position of the critical cis-proline 201.

$DsbG_{Q214R}$. Unlike K113N and V199A, the Q214R substitution is distant from the CXXC active site and is located at the surface of the DsbG cleft. The modeling suggests that the R214 guanidium group interacts (by hydrogen/ion–dipole interaction) with L195 backbone oxygen, in the C-terminus of helix α3, significantly diminishing the strength of the hydrogen bond (from wt = 3 Å to mutant Q214R = 3.3 Å). In DsbC, the Q214 position in DsbG is occupied by L192 that forms a hydrophobic cluster with L177 and a V179 in C-terminus of helix α3 (Fig. 4). We propose that the arginine side chain (longer than glutamine and composed of three aliphatic uncharged carbons) enlarges the hydrophobic surface of the DsbG cleft. This would modify the DsbG-substrate interaction and could enhance the ability of $DsbG_{Q214R}$ to recognize different unfolded proteins, as is the case for DsbC.

Taken together, the substitutions with profound effects on DsbG's activity are all predicted to weaken the intramolecular bonds within DsbG, especially around its active site.

Discussion

In this study, we introduce the use of a new yet simple blue/white genetic screen that can detect the disulfide bond isomerase activity *in vivo*. This screen is based on a serendipitously discovered mutant of alkaline phosphatase PhoA* that is dependent on DsbC for its folding and activity. We have used this screen to identify key residues involved in converting the sulfenic acid reductase DsbG into a disulfide bond isomerase that can rescue the isomerase defects in DsbC null mutants.

DsbC and DsbG are homologous proteins that are similar both in their structure and function. Their high level of similarities not surprisingly results in significant overlap in activities, yet they are sufficiently divergent as to have different substrate specificities. Overexpression of DsbG *in vivo* results in the correct folding of AppA and P1Lys (44) (data not shown), but not PhoA* or RNase I. On the other hand, DsbC is thought to assist in the folding of all the native *E. coli* substrates having nonconsecutive disulfide bonds and many eukaryotic proteins that are expressed recombinantly, suggesting significant functional differences between DsbC and DsbG. These differences in their substrate specificity may be due to differences in their CXXC active site pocket (27), known to modulate the activities of oxidoreductases (25). The active site residue K113 identified previously (14) and in our PhoA* screen here, along with the newly identified V199A, appears to be such a substitution modulating the activity of disulfide bond isomerases. Another difference between DsbC and DsbG is the electrostatic and structural make-up of their clefts. It has been assumed that the larger more charged cleft of DsbG plays a crucial role in modulating its activity and substrate specificity.

Through analyses of engineered DsbG* mutants with single amino acid substitutions, we discovered three mutations (Q214R, K113N, V199A) with profound effects on the activities of DsbG. These mutations are likely conferring isomerase activity on DsbG by either affecting DsbG-substrate interaction or DsbG active site reactivity. The substitution of glutamine 214 to arginine (Q214R) was sufficient to confer to DsbG* 50% of DsbC's ability to fold PhoA*. Glutamine 214 resides in the cleft of DsbG, assumed to be important in DsbG-substrate protein interaction. Computer modeling using PyMOL predicted that the longer side

chain of arginine would result in steric hindrance, causing the side chain of arginine to protrude into the cleft, likely affecting DsbG interaction with its substrate protein. The substitutions V199A and K113N are in close proximity to the CXXC active site, with K113 having direct hydrogen bonding with the active site cysteine 109, known to be involved in deprotonation of the resolving cysteine (31).

With certain substrates, DsbC can become engaged in a futile complex with a mis-oxidized protein that it cannot isomerize. When this occurs, DsbC requires an escape reaction. Otherwise, functional DsbC will be titrated out of the periplasmic space and new DsbC will need to be synthesized. DsbC can accomplish this escape reaction by reducing (instead of isomerizing) the mis-oxidized substrate, resulting in reduced substrate and oxidized DsbC. This may partially explain why DsbD is required to maintain DsbC in its active reduced state. These two models are not exclusive and are likely to coexist. In fact, correct folding of PhoA* can be achieved *in vivo* in the complete absence of any disulfide bond isomerase activity. We plated cells lacking *dsbC* and *dsbG* and expressing PhoA* on MOPS-XP plates with a filter disc in the middle of the plates, which we spotted with 10 μl of 1 *M* dithiothreitol (DTT). This resulted in a gradient of DTT away from the center of the filter disc. Surrounding the disc was a zone of inhibition where the concentration of DTT was too high to permit growth. However, immediately surrounding the zone of inhibition was a blue halo of cells with active correctly folded PhoA* (Supplementary Fig. S8). This result indicates that PhoA* can indeed fold correctly in the presence of DsbA and a chemical reductant, in the absence of any known disulfide bond isomerase. Analogously, the DsbC-dependent PDI detector can also form correct disulfide bonds and fold into its native state, in the absence of DsbC when supplemented with DTT (28). These observations support the model that cycles of oxidation/reduction can result in correct formation of disulfide bonds.

A number of our DsbG* variants confer resistance to copper overoxidation, in some cases up to the level seen for wt DsbC, which can function as an efficient reductase *in vitro* (50). DsbC has recently been shown to reduce the periplasmic copper-binding protein CueP *in vivo* (46). Similar to DsbG, DsbC is also a sulfenic acid reductase and maintains the single cysteine of the L-arabinose-binding protein AraF in its reduced state (5). The multiple *in vivo* roles of thiol oxidoreductases are apparently substrate dependent and can overlap. We favor a model in which DsbC not only isomerizes disulfide bonds but also reduces non-native disulfide bonds formed by copper oxidation, permitting reoxidation into native disulfide bonds by DsbA. Support for this model was shown *in vivo* by replacing the isomerization activity of DsbC by a dedicated reductase, resulting in correct folding of mis-oxidized proteins (38). Further support for the overlapping disulfide bond isomerase/reductase/oxidase activities of DsbG was shown through the *in vivo* oxidase activities of the DsbG* mutants isolated in this screen (Supplementary Fig. S7).

Oxidoreductases have previously been implicated in bestowing protection against metal-induced stress, resulting in their use in bioleaching processes (10). There is an intimate relationship between bioleaching organisms and oxidoreductases, as homologs of DsbC/G are frequently found in organisms resistant to metal-induced oxidative stress. For example, the DsbG homolog from *Acidithiobacillus ferrooxidans,* known for its capacity to grow in the presence of elevated metal concentrations, has been shown refold scrambled RNase A, unlike *E. coli* DsbG (48). Furthermore, a homolog of $DsbG^*_{KQ}$ (www.ncbi.nlm.nih.gov/protein/151283208?report=fasta) having the critical substitutions identified for both copper protection (K113N) and PhoA* isomerization (Q214R) is present in the sp. *Janthinobacterium marseille* HH01. *J. marseille* HH01 also encodes a remarkable number of proteins involved in resistance to drugs and heavy metals. Altogether, more than 2.4% of its genome is devoted to genes linked to resistance mechanisms (17). Yet, wt *E. coli* can grow efficiently at elevated levels of copper (9 m*M*), while *J. marseille* was shown to grow at a mere 0.6 m*M*. Most recently, DsbC from *Salmonella enterica* serovar typhimurium was shown to maintain the periplasmic copper-binding protein (CueP) in its reduced state (46). This recent finding not only further supports the role of DsbC in protecting cells from copper-induced toxicity but also shows that DsbC can indeed have a disulfide bond reductase function *in vivo*.

We have demonstrated the utility of the PhoA* screen to identify amino acid residues critical in modulating the activity and substrate specificity of DsbG. This screen can also be used to capture new protein-folding factors, chaperones, and oxidoreductases from various genetic sources (*e.g.*, from genomic libraries isolated from highly oxidizing environments) or to select for enzymes with modified oxidoreductase activities (*e.g.*, for DsbA mutants with higher fidelity in forming the correct disulfide bonds).

Materials and Methods

E. coli *strains, plasmids*

Bacterial strains and plasmids used in this work are described in Supplementary Table S4 and were constructed using standard molecular and genetic techniques (33).

Screening for DsbG capable of folding PhoA* on MOPS-XP plates*

We utilized the plasmid pMER79-*dsbG*-flag to construct a polymerase chain reaction (PCR) mutagenized library of *dsbG*s* protein-coding region using error prone PCR (GenScript). From the resulting library, we obtained random transformants on LB-Amp plates and subjected them to DNA sequencing. The majority of the plasmids (20/24) had inserts and, on an average, three nucleotide mutations per kilobase pair. Only the mature region of *dsbG* (devoid of its signal sequence) was PCR mutagenized and its cloning into the *Nco*I and *Xba*I (Cat. No. R3193 and R0145; NEB) restriction sites of pMER79 (38) resulted in a 5′ fusion to the SRP-dependent signal peptide (MRVLLFLLLSLFMLPAFS) of TorT protein (34) and a 3′ fusion to the FLAG-tag epitope. Converting the native signal sequence of DsbG to an SRP-dependent one allowed us to circumvent mutations that may alter the secretion of DsbG*. The carboxyl terminal flag tag allowed us to probe the *in vivo* redox state of DsbG*, independent of mutations that may alter the folding and immunoblot detection of DsbG*. Cells expressing periplasmic PhoA and grown on LB agar supplemented with XP can hydrolyze the phosphate moiety in XP, resulting in blue colonies (3). We used this enzymatic activity to develop a MOPS-XP-based screen, where XP was the sole phosphate

source. Thus, cells expressing active PhoA* can hydrolyze the phosphate moiety from XP, permitting growth. We transformed MB2272 strains carrying pBAD33-PhoA* with the plasmid library of mutagenized *dsbG** (pMER79-DsbG*-flag) and plated them on MOPS-XP selective media (1.5% agar, 1×MOPS [Cat. No. M2101; Teknova], 0.2% glycerol, 5 μM IPTG, 0.2% L-arabinose [Cat. No. A3256; Sigma], 2 mM L-glutathione reduced [GSH, Cat. No. G4251; Sigma], ampicillin [100 μg/ml], chloramphenicol [10 μg/ml], and 0.04 mg/ml XP [Cat. No. B6149; Sigma]), where XP was the sole phosphate source. Thus, strains expressing mutant DsbG* capable of folding PhoA* are able to hydrolyze the phosphate from XP, resulting in large blue colonies after 2 days at 30°C.

In vivo *PhoA* activity assay*

The PhoA* activity was determined *in vivo* by measuring the rate of pNPP hydrolysis. PhoA*, when correctly folded, hydrolyzes pNPP, leading to the formation of a yellow color that can be detected at 410 nm. Cells expressing PhoA* for ~18 h were grown at 30°C in minimal M63 media [3 g/L KH_2PO_4, 5.25 g/L K_2HPO_4, 1 g/L $(NH_4)_2SO_4$, 0.5 μg/L $FeSO_4$, 17 μg/ml 1×B1, and 1 mM $MgSO_4$] supplemented with 0.2% glycerol, 5 μM IPTG, 0.2% L-arabinose, and the selective antibiotics (ampicillin [100 μg/ml], chloramphenicol [10 μg/ml]). OD_{600} of the samples measured and standardized to 0.4. Twenty microliters of cells was mixed with 180 μl of the assay buffer (25 mM pNPP [Cat. No. N4645; Sigma], 1 mM zinc acetate in a 100 mM Tris buffer pH8) and the assay was performed in 96-well microtiter plates, measuring the rate of pNPP hydrolysis at 410 nm every 30 s for 2 h at 37°C. PhoA* enzymatic activity corresponds to the initial linear slope (V_{max}) calculated after 2 h. The experiments were conducted in duplicate, using two different biological samples.

In vivo *RNase I activity assay*

The RNase I activity was determined by measuring the rate of RNA hydrolysis in a methylene blue assay (9). Methylene blue intercalates into high-molecular-weight RNA, forming a complex that absorbs at 688 nm. When correctly folded, RNase I is active and hydrolyzes RNA molecules resulting in a decrease in absorbance at 688 nm. Cells expressing periplasmic RNase I were grown and induced overnight at 30°C in rich media supplemented with 0.2% L-arabinose, 5 μM IPTG, and the necessary antibiotics (ampicillin [100 μg/ml], chloramphenicol [10 μg/ml]). Cells were harvested, resuspended in MOPS media (Cat. No. M2101; Teknova), and sonicated. Using a Bradford assay, soluble protein concentrations of the samples were determined and standardized to $OD_{595} = 0.3$. Fifty microliters of samples was diluted to 1/100 with 150 μl of the assay buffer (methylene blue 1 g/L, yeast RNA 1 g/L [Cat. No. AM7118; Ambion], in 1×MOPS media), which had been preincubated for 10 min in the dark at 25°C. Change in absorbance at 688 nm was followed as a function of time at 25°C. Measured RNase I activity is the initial velocity determined after 300 s of reaction.

Copper toxicity rescue

Cells expressing *dsbC/dsbG/dsbG** from the plasmid pMER79 were grown in M63 media supplemented with 0.2% glycerol, the necessary antibiotics (100 μg/ml ampicillin, 10 μg/ml chloramphenicol), and 5 μM IPTG to mid-log phase and standardized to $OD_{600} = 0.4$. After diluting the samples from 10^0 to 10^{-4}, 5 μl of cells was spotted on BHI plates (52 g/L BHI, Cat. No. 211065; Becton, Dickinson and Company) supplemented with 2% agar, 100 μg/ml ampicillin, 10 μg/ml chloramphenicol, and 9 mM $CuSO_4$. After 2 days of incubation at 30°C, growth in the presence of copper was observed for some of the mutants.

DsbG CXXC active site redox state analysis

Cells expressing wt *dsbG* or mutant *dsbG*s* were grown in minimal M63 media supplemented with 0.2% glycerol, the necessary antibiotics (100 μg/ml ampicillin, 10 μg/ml chloramphenicol), and 5 μM IPTG. One milliliter cells $OD_{600} = 0.5$ were precipitated by incubating them with 50 μl of 100% trichloroacetic acid (TCA, Cat. No. A322-500; Thermo Fisher Scientific) on ice for 20 min. After pelleting the proteins at 14,000 rpm for 10 min, the proteins were washed with 500 μl ice-cold acetone for 20 min to remove excess TCA. Protein precipitate was spun for 10 min at 14,000 rpm and then air-dried at room temperature for 10 min. The pellet was resuspended in a 80 μl 4-acetamido-4′-maleimidylstilbene-2,2′-disulfonic acid (AMS) buffer (15 mM AMS [Cat. No. A485; Invitrogen], 1% sodium dodecyl sulfate (SDS), and 100 mM Tris HCl pH 8.0) using a shaker for 20 min at room temperature, followed by an incubation at 37°C for 40 min. To identify the oxidized and reduced states of DsbG, two controls were performed: (i) oxidized DsbG: the TCA precipitated pellet was resuspended in 80 μl of buffer without AMS (1% SDS, 100 mM Tris HCl pH 8.0) (ii) reduced DsbG: the TCA precipitated pellet was resuspended initially in a 200 μl DTT buffer (100 mM DTT [Cat. No. B7705; NEB], 1% SDS, 100 mM Tris HCl pH 8.0) for 20 min at room temperature under agitation. To the dissolved pellet, 600 μl minimal M63 media was added followed by TCA precipitation and AMS alkylation. A loading buffer (Cat. No. B7703; NEB) was added to the samples and boiled at 100°C for 10 min. Three microliter samples were loaded on a 10–20% SDS-PAGE tris-glycine polyacrylamide gel (Cat. No. 414893; CosmoBio). The gel was run for 75 min at 30 mA/gel. Proteins were transferred to a PVDF membrane (Cat. No. IPFL00010; Millipore). The blot was probed with rabbit polyclonal anti-FLAG antibodies (Cat. No. 2044S; Cell Signaling Technology) and detected using a secondary antibody coupled to an infrared dye (goat anti-rabbit IR Dye 800CW, Cat. No. 926-32211; Li-Cor).

*Purification of DsbG, DsbC, and DsbG*s*

DsbC, DsbG, and DsbG*s were purified using the pMAL protein fusion and expression system (Cat. No. E8200; NEB). A sequence encoding four alanines was inserted between *malE* and *dsbC/G/G** in the pMAL-c5X vector, as previous experiments with MBP-DsbC/DsbG/DsbG* showed that these fusions were resistant to cleavage with factor Xa. 3L of T7 Express Competent *E. coli* (Cat. No. C2566; NEB) containing the pMAL-c5X-dsbC/G/G* were grown at 37°C in rich media (5 g/L yeast extract, 10 g/L tryptone, 5 g/L sodium chloride, and 2 ml sodium hydroxide pH 7.2) supplemented with 0.2% glucose and the selective antibiotic (ampicillin 100 mg/ml). At $OD_{600} = 0.5$, MBP-DsbC/G/G* expression

was induced with 0.3 m*M* IPTG for 2 h at 37°C. Cells were harvested by centrifugation, resuspended in a 75 ml column buffer (CB) (20 m*M* Tris-HCl pH 7.4, 0.2 *M* NaCl, 1 m*M* ethylenediaminetetraacetic acid [EDTA]), and frozen at −20°C overnight. The cell suspension was thawed, lysed by sonication, and centrifuged to obtain the soluble fraction. The crude extract was diluted 1:6 with CB. The crude fraction was applied to a 5 × 2-cm column containing 40 ml amylose resin (Cat. No. E8021; NEB). The column was washed with 250 ml CB, and the MBP-DsbC/G/G* fusion protein was eluted with 250 ml water. Using a Vivaspin 30 concentrator (Cat. No. VS2022; Sartorius), the eluted protein was concentrated to ~1 mg/ml by ultrafiltration using the Vivaspin 30 concentrator (Cat. No. VS2022; Sartorius). A Factor Xa buffer was added to a final concentration of 20 m*M* Tris-HCl pH 8, 100 m*M* NaCl, 0.2 m*M* $CaCl_2$, and the fusion protein was digested at room temperature for 24 h with 1% factor Xa (Cat. No. P8010; NEB). The cleavage mixture was loaded on the same amylose column used for the first step. The flow-through was collected and run through a HiTrap benzamidine FF column (Cat. No. 17-5143-01; GE Healthcare). The column flow-through was concentrated to 5 mg/ml, dialyzed into a 10 m*M* HEPES buffer pH 7.5, and stored at −20°C.

In vitro *oxidoreductase assays*

Disulfide bond reductase assay. The two polypeptides of insulin (A and B) are covalently linked by a disulfide bond. The reduction of insulin results in the precipitation of the protein, which can be monitored in a spectrophotometer. The ability of DsbC, DsbG, and variants to catalyze the reduction of human insulin in the presence of DTT was tested as described previously (16). A stock solution of 872 μM insulin was freshly prepared in a 0.1 *M* Tris buffer, pH ~7.0, and 1 m*M* EDTA before each assay. The reaction mixtures were prepared directly in cuvettes using a 0.1 *M* sodium phosphate buffer, pH 7.0, 1 m*M* EDTA, and 0.33 m*M* DTT with 10 μM enzyme in a final volume of 0.75 ml. Adding insulin to a final concentration of 131 μM started the reactions. After thoroughly mixing, the cuvettes were placed in the spectrophotometer and measurements were performed at 650 nm for 120 min. In all experiments, the uncatalyzed reduction of insulin by DTT was monitored in a control reaction without the addition of enzymes.

Disulfide bond oxidase assay. The oxidative folding of hirudin was tested as described previously (27). In brief, the oxidase activity was determined by the rate at which 0.5 μM oxidized DsbG or variants donate a disulfide bond to reduced hirudin (ranging from 1 to 2.5 μM). The buffer was nitrogen saturated. The fluorescence excitation at 295 nm increases when oxidized DsbG or DsbG* loses its active site disulfide bond; however, hirudin itself shows no fluorescence change during the reaction. The assay was performed on a Hitachi F-4500 fluorescence spectrophotometer in the single-mixing mode. The traces were fit individually to a single exponential equation to obtain the pseudofirst-order rate constant Kobs. Averaged Kobs values were plotted against the hirudin concentration. The slope is the observed second-order rate constant of the reaction.

Disulfide bond isomerase assay. The scrambled hirudin refolding assay was conducted as described previously (23). Hirudin (Botai Ltd.) samples were diluted to 24 μM and incubated with or without 24 μM reduced DsbC, DsbG, or DsbG variants in 100 m*M* sodium phosphate, 1 m*M* EDTA, pH 7.0. Following incubation at room temperature at various time points, folding reactions were quenched by addition of 10% (v/v) formic acid. Buffer was nitrogen saturated. The reaction products were separated by reverse-phase HPLC on a VydacTM218TP54 C18 column at 55°C using an acetonitrile gradient (19–25%, 30 ml) in 0.1% (v/v) trifluoroacetic acid. The eluted proteins were detected by their absorbance at 220 nm. The activity was quantified by the ratio of native folded hirudin peak area *versus* all hirudin peaks after the reaction quenched at 17 h. The ratio of DsbC catalyzed reaction was set to 100%, while all DsbG* catalyzed reactions were normalized to wt DsbC to represent the DsbG*isomerase activity. Noncatalyzed reaction was used as the negative control.

Bioinformatic analysis of DsbC and DsbG homologs

Using 11 DsbC and 20 DsbG homologs with 99–100% sequence identity to *E. coli* DsbC and DsbG, homologs were selected from BLAST results. The homologs were aligned using ClustalW2 (www.ebi.ac.uk/Tools/msa/clustalw2/). The alignments were used to generate two hidden Markov models using Hmmer3's hmmbuild function (http://hmmer.janelia.org). Hmmer3's hmmsearch function was used to search for proteins within a database of 816 bacterial and archaeal genomes downloaded on March 14, 2009, from NCBI (ftp://ftp.ncbi.nlm.nih.gov/genbank/genomes/Bacteria/) that match the models with a sequence E-value threshold $\leq 1e^{-05}$. The matched sequences were aligned with muscle (www.ebi.ac.uk/Tools/msa/muscle/) and trimmed to remove poorly aligned regions. Two methods, trimAL (http://trimal.cgenomics.org) and Gblocks (http://molevol.cmima.csic.es/castresana/Gblocks.html), produced similar results. A tree was generated using PhyML (www.atgc-montpellier.fr/phyml/). Prediction of protein topology using Phobius (http://phobius.binf.ku.dk) and conserved residues of DsbC and DsbG homologs using ConSurf (http://consurftest.tau.ac.il) were performed. Finally, the tree was visualized using iTol (http://itol.embl.de). Alignment of DsbC and DsbG was performed by the CEAlign tool in PyMOL, based on the combinatorial extension algorithm (37).

Homology modeling of DsbG mutants. DsbG K113N, Q214R, V199A, and KQ mutants were modeled from DsbG crystal structure (PDB 1V57) (11) using Modeler 9.13 (32), as described in the Modeler tutorial (basic modeling). Fifty homology models were built and the best were selected. Residues of the thioredoxin domain (88–230) were selected for further refinement. Minimization: protein solvation and minimization steps were performed using the Molecular Modeling ToolKit (MMTK) (15). Step 1: Protonation → Protonation state of homology models was set at pH 7, according to the standard setting in MMTK. Next steps were run on the reduced form of the thioredoxin domain. Step 2: Solvation → Homology models were loaded into orthorhombic periodic boxes twofold larger than model eigenvalues. Model coordinates were fixed to prevent model deformation during the solvation process. Explicit water molecules were randomly added to reach a density of 1 g/cm^3, without molecules overlapping. Using the Amber99 force field (43), the solvent was equilibrated for 1000

steps at 300 K and 1 atm. Lenard jones (LJ) and electrostatic (El) cutoffs were set to 7 Å and 4 Å, respectively. The solvent was minimized around homology models until a convergence of $5e^{-3}$, using a steepest descent minimization. Step 3: Minimization → Homology model coordinates were unfixed. LJ cutoff was set to 10 Å, and El cutoff was computed using Ewald summation. Both solvent and homology models were minimized until a convergence of $5e^{-3}$, using a conjugate gradient minimization.

Acknowledgments

We would like to thank Koreaki Ito, Iris Walker, and Melanie Berkmen for the critical reading of the article and Vladimir Potapov for his helpful advice on molecular modeling.

Author Disclosure Statement

No competing financial interests exist.

References

1. Berkmen M, Boyd D, and Beckwith J. The nonconsecutive disulfide bond of *Escherichia coli* phytase (AppA) renders it dependent on the protein-disulfide isomerase, DsbC. *J Biol Chem* 280: 11387–11394, 2005.
2. Bessette PH, Cotto JJ, Gilbert HF, and Georgiou G. *In vivo* and *in vitro* function of the *Escherichia coli* periplasmic cysteine oxidoreductase DsbG. *J Biol Chem* 274: 7784–7792, 1999.
3. Brickman E and Beckwith J. Analysis of the regulation of *Escherichia coli* alkaline phosphatase synthesis using deletions and phi80 transducing phages. *J Mol Biol* 96: 307–316, 1975.
4. Collet JF and Messens J. Structure, function, and mechanism of thioredoxin proteins. *Antioxid Redox Signal* 13: 1205–1216, 2010.
5. Denoncin K, Vertommen D, Arts IS, Goemans CV, Rahuel-Clermont S, Messens J, and Collet JF. A new role for *Escherichia coli* DsbC in protection against oxidative stress. *J Biol Chem* 289: 12356–12364, 2014.
6. Depuydt M, Leonard SE, Vertommen D, Denoncin K, Morsomme P, Wahni K, Messens J, Carroll KS, and Collet JF. A periplasmic reducing system protects single cysteine residues from oxidation. *Science* 326: 1109–1111, 2009.
7. Dyson HJ, Jeng MF, Tennant LL, Slaby I, Lindell M, Cui DS, Kuprin S, and Holmgren A. Effects of buried charged groups on cysteine thiol ionization and reactivity in *Escherichia coli* thioredoxin: structural and functional characterization of mutants of Asp 26 and Lys 57. *Biochemistry* 36: 2622–2636, 1997.
8. Gleiter S and Bardwell JC. Disulfide bond isomerization in prokaryotes. *Biochim Biophys Acta* 1783: 530–534, 2008.
9. Greiner-Stoeffele T, Grunow M, and Hahn U. A general ribonuclease assay using methylene blue. *Anal Biochem* 240: 24–28, 1996.
10. Hayashi S, Abe M, Kimoto M, Furukawa S, and Nakazawa T. The *dsbA-dsbB* disulfide bond formation system of *Burkholderia cepacia* is involved in the production of protease and alkaline phosphatase, motility, metal resistance, and multi-drug resistance. *Microbiol Immunol* 44: 41–50, 2000.
11. Heras B, Edeling MA, Schirra HJ, Raina S, and Martin JL. Crystal structures of the DsbG disulfide isomerase reveal an unstable disulfide. *Proc Natl Acad Sci U S A* 101: 8876–8881, 2004.
12. Hiniker A and Bardwell JC. *In vivo* substrate specificity of periplasmic disulfide oxidoreductases. *J Biol Chem* 279: 12967–12973, 2004.
13. Hiniker A, Collet JF, and Bardwell JC. Copper stress causes an *in vivo* requirement for the *Escherichia coli* disulfide isomerase DsbC. *J Biol Chem* 280: 33785–33791, 2005.
14. Hiniker A, Ren G, Heras B, Zheng Y, Laurinec S, Jobson RW, Stuckey JA, Martin JL, and Bardwell JC. Laboratory evolution of one disulfide isomerase to resemble another. *Proc Natl Acad Sci U S A* 104: 11670–11675, 2007.
15. Hinsen K. The Molecular Modeling Toolkit: a new approach to molecular simulations. *J Comp Chem* 21: 79–85, 2000.
16. Holmgren A. Thioredoxin catalyzes the reduction of insulin disulfides by dithiothreitol and dihydrolipoamide. *J Biol Chem* 254: 9627–9632, 1979.
17. Hornung C, Poehlein A, Haack FS, Schmidt M, Dierking K, Pohlen A, Schulenburg H, Blokesch M, Plener L, Jung K, Bonge A, Krohn-Molt I, Utpatel C, Timmermann G, Spieck E, Pommerening-Roser A, Bode E, Bode HB, Daniel R, Schmeisser C, and Streit WR. The *Janthinobacterium* sp. HH01 genome encodes a homologue of the *V. cholerae* CqsA and *L. pneumophila* LqsA autoinducer synthases. *PLoS One* 8: e55045, 2013.
18. Kadokura H and Beckwith J. Mechanisms of oxidative protein folding in the bacterial cell envelope. *Antioxid Redox Signal* 13: 1231–1246, 2010.
19. Kadokura H, Tian H, Zander T, Bardwell JC, and Beckwith J. Snapshots of DsbA in action: detection of proteins in the process of oxidative folding. *Science* 303: 534–537, 2004.
20. Kong B and Guo GL. Soluble expression of disulfide bond containing proteins FGF15 and FGF19 in the cytoplasm of *Escherichia coli*. *PLoS One* 9: e85890, 2014.
21. Kurokawa Y, Yanagi H, and Yura T. Overexpression of protein disulfide isomerase DsbC stabilizes multiple-disulfide-bonded recombinant protein produced and transported to the periplasm in *Escherichia coli*. *Appl Environ Microbiol* 66: 3960–3965, 2000.
22. Lobstein J, Emrich CA, Jeans C, Faulkner M, Riggs P, and Berkmen M. SHuffle, a novel *Escherichia coli* protein expression strain capable of correctly folding disulfide bonded proteins in its cytoplasm. *Microb Cell Fact* 11: 56, 2012.
23. Lu BY and Chang JY. Assay of disulfide oxidase and isomerase based on the model of hirudin folding. *Anal Biochem* 339: 94–103, 2005.
24. Masip L, Klein-Marcuschamer D, Quan S, Bardwell JC, and Georgiou G. Laboratory evolution of *Escherichia coli* thioredoxin for enhanced catalysis of protein oxidation in the periplasm reveals a phylogenetically conserved substrate specificity determinant. *J Biol Chem* 283: 840–848, 2008.
25. Mavridou DA, Saridakis E, Kritsiligkou P, Mozley EC, Ferguson SJ, and Redfield C. An extended active-site motif controls the reactivity of the thioredoxin fold. *J Biol Chem* 289: 8681–8696, 2014.
26. Messens J, Collet JF, Van Belle K, Brosens E, Loris R, and Wyns L. The oxidase DsbA folds a protein with a nonconsecutive disulfide. *J Biol Chem* 282: 31302–31307, 2007.
27. Quan S, Schneider I, Pan J, Von Hacht A, and Bardwell JC. The CXXC motif is more than a redox rheostat. *J Biol Chem* 282: 28823–28833, 2007.
28. Ren G and Bardwell JC. Engineered pathways for correct disulfide bond oxidation. *Antioxid Redox Signal* 14: 2399–2412, 2011.

29. Ren G, Stephan D, Xu Z, Zheng Y, Tang D, Harrison RS, Kurz M, Jarrott R, Shouldice SR, Hiniker A, Martin JL, Heras B, and Bardwell JC. Properties of the thioredoxin fold superfamily are modulated by a single amino acid residue. *J Biol Chem* 284: 10150–10159, 2009.
30. Rensing C and Grass G. *Escherichia coli* mechanisms of copper homeostasis in a changing environment. *FEMS Microbiol Rev* 27: 197–213, 2003.
31. Rohr AK, Hammerstad M, and Andersson KK. Tuning of thioredoxin redox properties by intramolecular hydrogen bonds. *PLoS One* 8: e69411, 2013.
32. Sali A and Blundell TL. Comparative protein modelling by satisfaction of spatial restraints. *J Mol Biol* 234: 779–815, 1993.
33. Sambrook J, Fritsch EF, and Maniatis T. *Molecular Cloning: A Laboratory Manual.* Cold Spring Harbor, NY: Cold Spring Harbor Laboratory, 1989.
34. Schierle CF, Berkmen M, Huber D, Kumamoto C, Boyd D, and Beckwith J. The DsbA signal sequence directs efficient, cotranslational export of passenger proteins to the *Escherichia coli* periplasm via the signal recognition particle pathway. *J Bacteriol* 185: 5706–5713, 2003.
35. Schrödinger. The PyMOL Molecular Graphics System, LLC. Version 1.2r3pre.
36. Shao F, Bader MW, Jakob U, and Bardwell JC. DsbG, a protein disulfide isomerase with chaperone activity. *J Biol Chem* 275: 13349–13352, 2000.
37. Shindyalov IN and Bourne PE. Protein structure alignment by incremental combinatorial extension (CE) of the optimal path. *Protein Eng* 11: 739–747, 1998.
38. Shouldice SR, Cho SH, Boyd D, Heras B, Eser M, Beckwith J, Riggs P, Martin JL, and Berkmen M. *In vivo* oxidative protein folding can be facilitated by oxidation-reduction cycling. *Mol Microbiol* 75: 13–28, 2010.
39. Sone M, Akiyama Y, and Ito K. Differential *in vivo* roles played by DsbA and DsbC in the formation of protein disulfide bonds. *J Biol Chem* 272: 10349–10352, 1997.
40. Sone M, Akiyama Y, and Ito K. Additions and corrections: differential *in vivo* roles played by DsbA and DsbC in the formation of protein disulfide bonds. *J Biol Chem* 273: 27756, 1998.
41. Sone M, Kishigami S, Yoshihisa T, and Ito K. Roles of disulfide bonds in bacterial alkaline phosphatase. *J Biol Chem* 272: 6174–6178, 1997.
42. Torrentó C, Cama J, Urmenetab J, Oteroc N, and Solerc A. Denitrification of groundwater with pyrite and *Thiobacillus denitrificans*. *Chem Geol* 278: 80–91, 2010.
43. Wang J, Cieplak P, and Kollman PA. How well does a restrained electrostatic potential (RESP) model perform in calculating conformational energies of organic and biological molecules? *J Comp Chem* 21: 1049–1074, 2000.
44. Xu M, Arulandu A, Struck DK, Swanson S, Sacchettini JC, and Young R. Disulfide isomerization after membrane release of its SAR domain activates P1 lysozyme. *Science* 307: 113–117, 2005.
45. Yang J, Kanter G, Voloshin A, Levy R, and Swartz JR. Expression of active murine granulocyte-macrophage colony-stimulating factor in an *Escherichia coli* cell-free system. *Biotechnol Prog* 20: 1689–1696, 2004.
46. Yoon BY, Kim JS, Um SH, Jo I, Yoo JW, Lee K, Kim YH, and Ha NC. Periplasmic disulfide isomerase DsbC is involved in the reduction of copper binding protein CueP from *Salmonella enterica serovar Typhimurium*. *Biochem Biophys Res Commun* 446: 971–976, 2014.
47. Zapun A, Missiakas D, Raina S, and Creighton TE. Structural and functional characterization of DsbC, a protein involved in disulfide bond formation in *Escherichia coli*. *Biochemistry* 34: 5075–5089, 1995.
48. Zhang CG, Xia JI, Liu YD, He H, and Qiu GZ. The putative thiol-disulphide interchange protein DsbG from *Acidithiobacillus ferrooxidans* has disulphide isomerase activity. *ScienceAsia* 36: 100–104, 2010.
49. Zhang Z, Li ZH, Wang F, Fang M, Yin CC, Zhou ZY, Lin Q, and Huang HL. Overexpression of DsbC and DsbG markedly improves soluble and functional expression of single-chain Fv antibodies in *Escherichia coli*. *Protein Expr Purif* 26: 218–228, 2002.
50. Zhao Z, Peng Y, Hao SF, Zeng ZH, and Wang CC. Dimerization by domain hybridization bestows chaperone and isomerase activities. *J Biol Chem* 278: 43292–43298, 2003.
51. Zheng M, Wang X, Doan B, Lewis KA, Schneider TD, and Storz G. Computation-directed identification of OxyR DNA binding sites in *Escherichia coli*. *J Bacteriol* 183: 4571–4579, 2001.
52. Zheng M, Wang X, Templeton LJ, Smulski DR, LaRossa RA, and Storz G. DNA microarray-mediated transcriptional profiling of the *Escherichia coli* response to hydrogen peroxide. *J Bacteriol* 183: 4562–4570, 2001.

Address correspondence to:
Dr. Mehmet Berkmen
Protein Expression and Modification
New England Biolabs
240 County Road
Ipswich, MA 01938

E-mail: berkmen@neb.com

Date of first submission to ARS Central, December 22, 2014; date of final revised submission, April 28, 2015; date of acceptance, May 13, 2015.

Abbreviations Used

AMS = 4-acetamido-4′-maleimidylstilbene-2,2′-disulfonic acid
BHI = brain heart infusion
CB = column buffer
DTT = dithiothreitol
EDTA = ethylenediaminetetraacetic acid
GSH = L-glutathione reduced
HPLC = high-performance liquid chromatography
LJ = Lenard jones
MOPS = 3-(*N*-morpholino)propanesulfonic acid
PCR = polymerase chain reaction
pNPP = 4-nitrophenyl phosphate
PVDF = polyvinylidene fluoride
RNase I = ribonuclease I
SDS = sodium dodecyl sulfate
SDS-PAGE = sodium dodecyl sulfate–polyacrylamide gel electrophoresis
SRP = signal recognition particle
TCA = trichloroacetic acid
wt = wild type
XP = 5-bromo-4-chloro-3-indolyl phosphate